Experimental results from the cryogenic cooling of a rotor using an internal pump

Experimental results from the cryogenic cooling of a rotor using an internal pump

A J Caughley[1*], G Lumsden[2], R Badcock[2], M Gschwendtner[3] and S Jeong[4]

[1] Callaghan Innovation, 5 Sheffield Crescent, Christchurch 8053, New Zealand
[2] Robinson Research Institute, Victoria University of Wellington, Lower Hutt, 5010 New Zealand
[3] AUT University, 55 Wellesley St E, Auckland, 1010, New Zealand
[4] Korea Advanced Institute of Science and Technology, Daejeon 34141, Republic of Korea

[*]E-mail: alan.caughley@callaghaninnovation.govt.nz

Abstract. Superconducting motors are a route to the high power-to-weight ratio required for the electrification of large aircraft. In a synchronous superconducting motor, a popular configuration is to have the rotor with DC field coils and the stator with AC coils. This configuration makes the rotor cooling easier, as DC superconducting coils have few losses. However, the heat from the rotor still needs to be transferred across a high-speed rotating interface. Our proposed cooling method uses a helium gas circuit, internal to the rotor, that is circulated by the rotor's motion against that of a cold stationary heat exchanger. Keeping the cold heat exchanger stationary reduces sealing requirements as the internally pumped gas can be kept near ambient pressure whilst the cold heat exchanger could be cooled by either pressurised cryogenic fluid, a two-phase medium, or a cryocooler. The internal rotor pump concept was first validated with a CFD model, which was in turn confirmed by experimentation. This paper presents the results of the proof-of-concept experiments that validated the CFD model and will present further improvements to the concept, demonstrating a feasible cooling method and its application to a superconducting rotor.

1. Introduction

Electrification of air travel requires a drive train with a very high power-density to compete with gas turbines. Superconducting motors have been proposed as a way to achieve the power densities required for aviation, as they are light and compact. Superconductors however, work at cryogenic temperatures which indispensably would require a light, reliable and efficient cooling mechanism to be implemented on an aircraft. Additionally, the removal of heat from a cryogenic spinning rotor to a cryocooler presents a significant challenge. Previous motors have utilized cryogenic coolants in the form of pumped gaseous helium [1–5] or thermo-syphoned cryogens [5–8] to transfer heat from the rotor to a cryocooler. Transferring a cryogen across a spinning interface rotor requires rotary seals, usually ferro-fluidic seals [6] as they have a very low leak rate. The aircraft application demands a compact and low weight solution. Moreover, aircraft propulsion fans run at high speeds. Ferrofluidic seals are not compact and generate significant amounts of heat at high shaft speeds due to the thick oil used as the seal. The additional cooling and thermal isolation from the cryogenic environment are undesirable in an aircraft application. Jeong [9] and Dyson [10] proposed mounting the cryocooler on the rotor, rotating with it. Jeong

proved experimentally that spinning did not affect the performance of a pulse tube cryocooler. However, potential difficulties with spinning the cryocooler involve the addition of a large spinning mass (the cryocooler) to the rotor, transferring electrical power to the cryocooler and removing heat from the cryocooler. The advantage of rotating the cryocooler is that heat transfer across the rotating/stationary interface would happen at an ambient temperature, the disadvantage is that the amount of heat to be transferred is much greater as it is in the order of 1 kW at 300 K rather than the 20-50 W to be removed at 50 K.

The Robinson Research Institute (RRI) is developing a 3 MW superconducting motor using a High Temperature Superconductor (HTS) rotor operating at 50 K and a stator wound with MgB2 at near 20 K. The motor is intended to run at a shaft speed of 4500-6000 rpm to directly drive a ducted fan. Initially RRI will build a 100-kW prototype to test key aspects of the concept, being the power electronics, the rotor and its cooling, and the stator with its cooling. The 100 kW prototype's rotor will be the same size as the 3 MW motor, being 200 mm in diameter and 400 mm long. RRI's calculations are that the rotor will nominally require 20-50 W cooling at 50 K [11].

A concept was developed for utilising a stationary heat exchanger inside a spinning rotor to circulate cold helium gas past the heat exchanger and around the rotor [11]. A shortened rotor prototype was designed to test the concept. Initial CFD modelling predicted that the rotor would have a heat load of 16 W at 50 K and that the circulated gas could transfer the heat to a heat exchanger on a SunPower DS30 cryocooler with a temperature difference of 2.5 K between the coil section of the rotor and the cold heat exchanger. This equates to a conductance of 6.4 W/K. It was postulated that keeping the helium gas slightly above atmospheric and using high performance Trelleborg lip seals would give sufficient sealing to stop ingress of air and reduce helium loss to an acceptable amount. A prototype of the CFD model was constructed and tested.

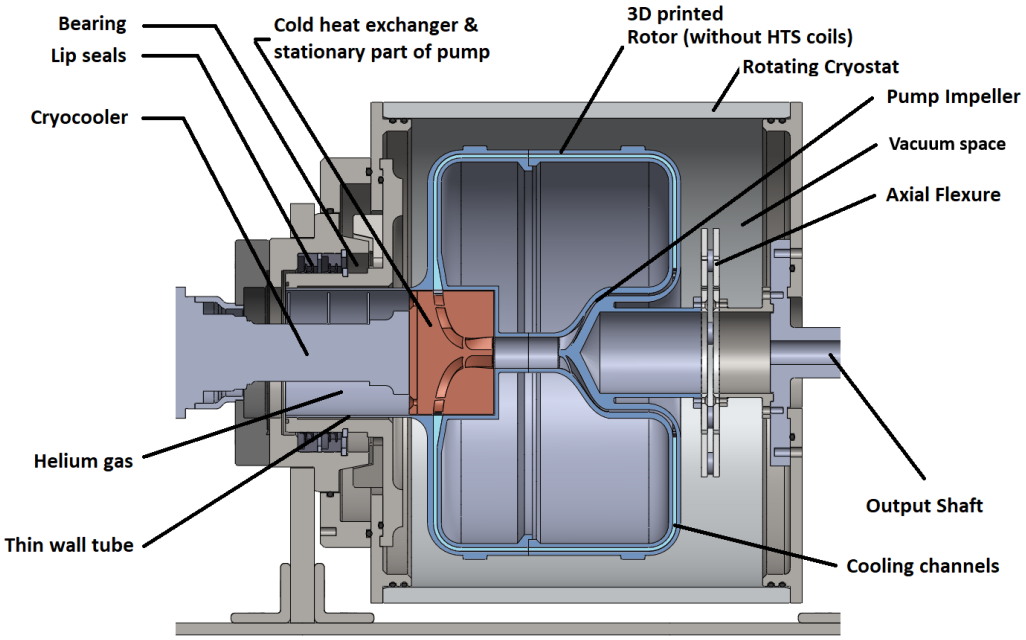

Figure 1. Layout of test rotor. The test rotor is a shortened version of the 100-kW rotor. The cryocooler is on the left and the drive output shaft on the right.

Stationary cool-down and warm-up transients confirmed the modelled heat load [12]. Temperature profiles during cooling while stationary confirmed the CFD model's prediction of gravity-driven natural convection being the dominant heat transfer mechanism. The leakage of the lip seas was manageable, corresponding to a leakage rate of 0.6 standard litres of gas per hour.

The experimental rig, while stationary, reached an average rotor temperature of 88 K with the cryocooler at 62 K, corresponding to a heat load of 16 W. The best conductance measured between the cryocooler and the coil section of the rotor was 0.62 W/K. This paper presents results of rotating tests showing the effect of the pumping and of improvements to the system to increase the conductance, especially with a stationary rotor. The hypothesis being that, once rotating, the pumping effect would change the flow pattern in the rotor from the stationary situation, which would be evident in the temperatures around the rotor, with the coldest sensors at the driveshaft end and warmest at the cryocooler end.

2. Experiments

The shortened rotor test rig consisted of a 3D-printed stainless-steel rotor inside a rotating cryostat with the cryocooler cold head stationary inside the rotor, as in Figure 1. Eight PT100 temperature sensors were fixed to the rotor in positions as in Figure 2. The sensor wires were fed through the shaft to a low power processor, to convert to voltages which were sent to the stationary domain via an infrared link. The rotating tests were conducted with a static vacuum in the rotor cryostat as the rig did not have a rotary connection for continuous vacuum pumping. The rotor test rig is described fully in reference [12].

2.1 Rotating test demonstrating proof of concept

The rotating test temperatures are shown Figure 3. The rotating test started with a stationary cooldown to reach steady state with the rotor reaching an average temperature of 92.8 K and the cryocooler 63 K. The temperature patterns were consistent with convection from density-driven currents. Rotation was started at 1000 rpm. The target speed was 4500 rpm, but a lower speed

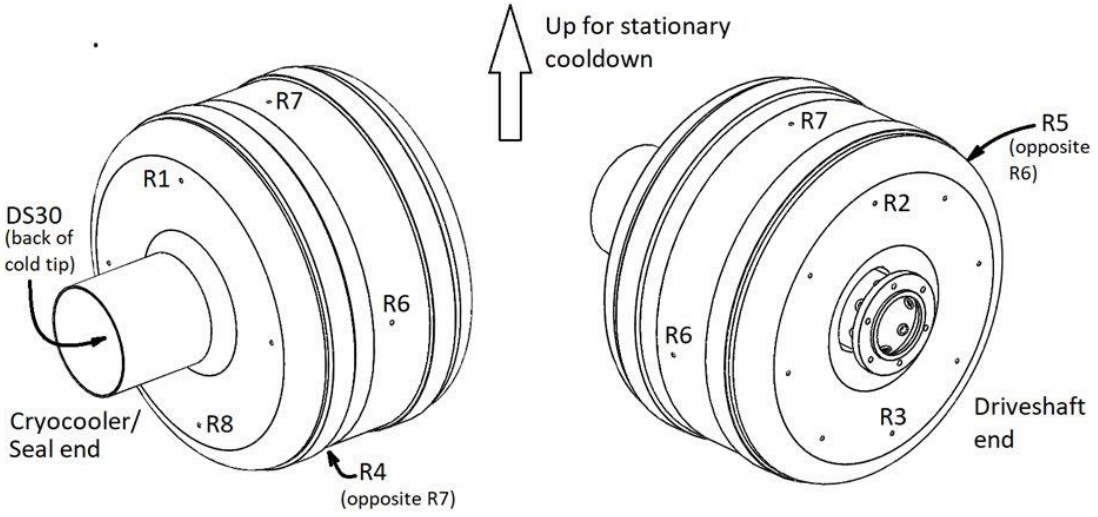

Figure 2. Positions of temperature sensors R1 to R8 on the Rotor.

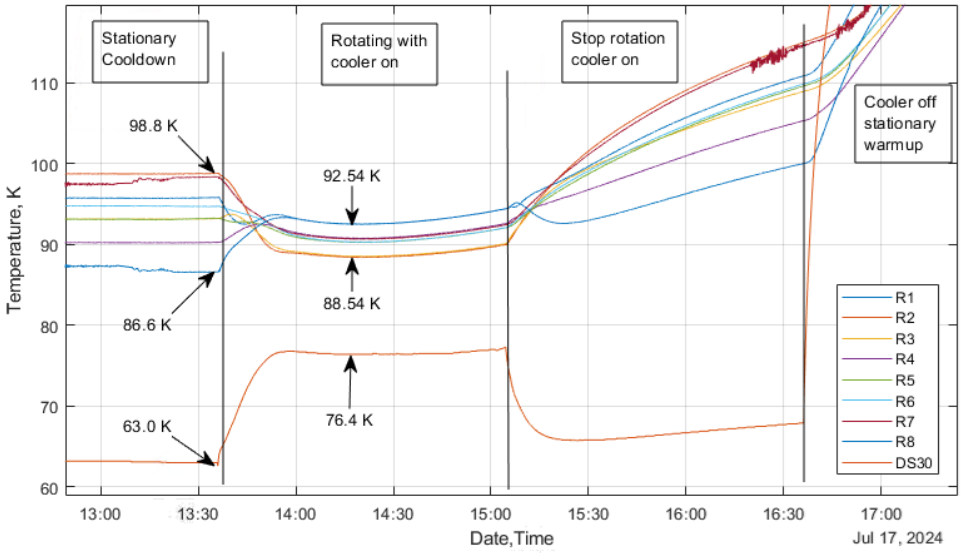

Figure 3. Rotor and cryocooler temperature measurements for the rotating test.

was chosen to reduce the heat generation by the lip seals, which had more frictional resistance than anticipated. Rotation continued for approximately 80 minutes, attaining a pseudo steady state temperature distribution. Initially the rotor temperature reduced, then added heat from vacuum deterioration in the rotor cryostat overcame the refrigeration effect and the temperature started to rise. The rotation was stopped with the cryocooler continuing, the warming rate increased due to the deteriorated vacuum and poorer conductance while stationary. Finally, the cryocooler was turned off and the system allowed to warm up. As hypothesised, Figure 3 shows that whilst stationary the coldest temperatures of the rotor were R8 and R4, the lowest two sensors, which were cooled by gravity driven convection currents. Conversely, the warmest sensors, R2 and R7, were at the top of the rotor. When rotation started, the CFD modelling predicted that the flow of cold gas from the heat exchanger to the driveshaft end of the rotor would make the sensors R2 and R3 the coldest. The warmest sensors would be R1 and R8 at the cryocooler end of the rotor where the gas re-entered the heat exchanger after picking up the heat from the rotor. This transition of temperatures was experimentally observed showing the cooling from the pumping action. Additionally, the cryocooler temperature increased while the rotor temperatures decreased, indicating a higher heat load on the cryocooler as it first cooled the rotor then worked against the increased heat load. At the best point, the rotor was cooled to an average of 90.5K. Cooling whilst stationary achieved an average rotor temperature of 92.8 K from a cryocooler at 63 K with 16 W of heat load, corresponding to a total conductance of 0.54 W/K heat transfer. When rotation started, the rotor average temperature dropped to 90.5 K from a cryocooler temperature of 76.4 K. The heat load, as calculated from the cryocooler's measured cooling curve [12], increased to 25 W due to the vacuum deterioration in the rotor. The resulting conductance was 1.76 W/K and demonstrates improved heat transfer from the pumping effect.

The heat capacity of helium at 1.2 bara and 85 K is 5.19 kJ/kg.K. A temperature rise of 14.4 K in the gas (warmest part of rotor to cryocooler) for 16 W of heat load (25 W total minus 10 W from the bearing end which is not intercepted by the flow) implies a mass flow of 0.2 g/s. The CFD model was rerun at 1000 rpm with the cryocooler at 76.4 K and 25 W total heat load. It calculated

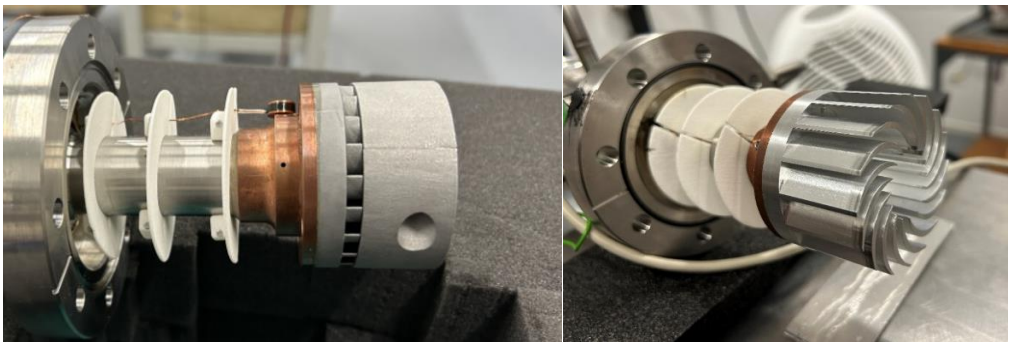

Figure 4. Left, the original 3D printed heat exchanger, and right the new heat exchanger with increased heat transfer area. Both mounted on the cryocooler.

0.24 g/s mass flow rate with a rotor temperature of 97 K. The experiment performed better than the CFD model's prediction [11], implying that it would do better than the CFD predicted conductance of 6 W/K at 4500 rpm.

2.2 Improvements to the cold heat exchanger

The effective conductance with the original design while stationary was 0.62 W/K [12]. For a 20 W cooling load, this would result in an unacceptable temperature difference of 40 K between the cold heat exchanger and the rotor. The original shape of the heat exchanger followed the gas flow path within heat exchanger while rotating. This gave a smooth flow but lacked area for cooling while stationary. An alternative heat exchanger, shown in Figure 4, was designed to increase the heat exchange area by filling the available cylindrical space with vanes while keeping the inlet and exit angles for the flow when rotating. The larger area would enable the gas to reach a colder temperature before circulating through the rotor.

The CFD model of the new design, shown in Figure 5, predicted a lower over-all temperature of the rotor while stationary, and a similar temperature while rotating. The predicted flow path

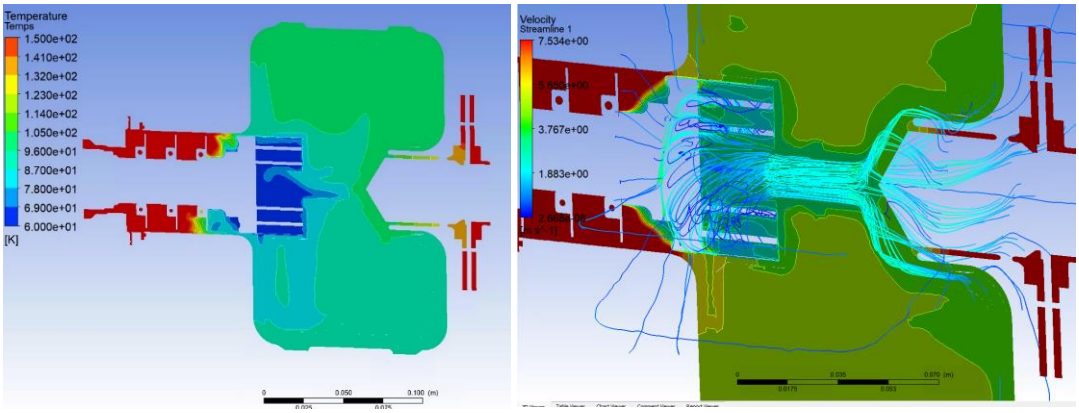

Figure 5. CFD model of the new heat exchanger design showing the temperature profiles and velocity streamlines through the heat exchanger. Left is cooling of the rotor whilst stationary, showing the gravitational convection inside the rotor. Right is whilst rotating, showing the streamlines from the pumping action and flow through the heat exchanger.

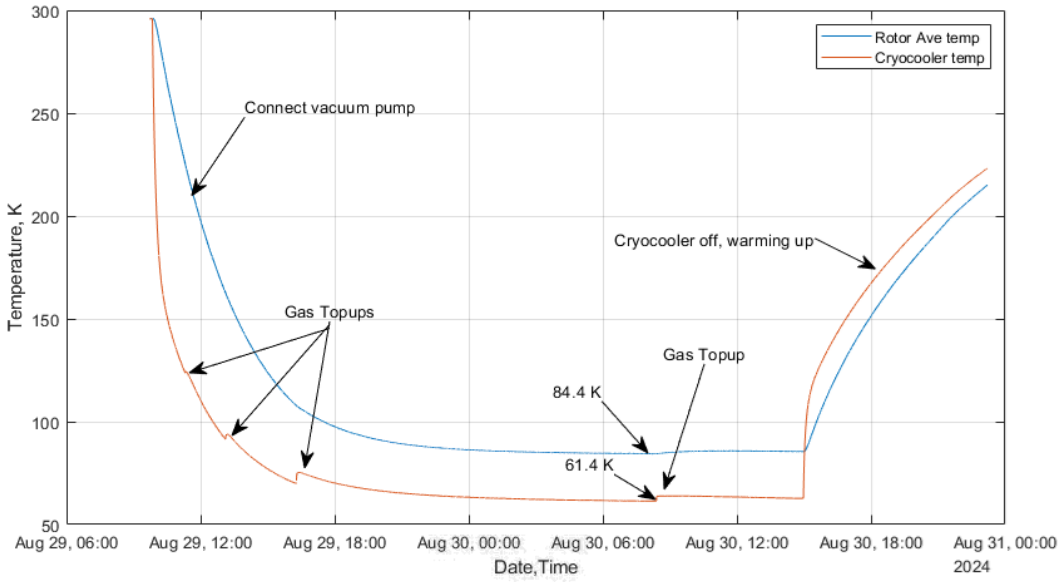

Figure 6. Rotor average and cryocooler temperatures for a stationary cool down with the new cold heat exchanger.

through the rotor, while rotating, was very similar to the previous heat exchanger. The stationary cooldown test with the new heat exchanger is shown in Figure 6. The average rotor temperature, while stationary, dropped to 84.4 K with the cryocooler at 61.4 K, a marked improvement from the previous 92.8 K and corresponds to a conductance of 0.75 W/K.

The rotation test for the new heat exchanger is shown in Figure 7. The test started from steady state while stationary, the vacuum pump was disconnected and rotation started at 1000

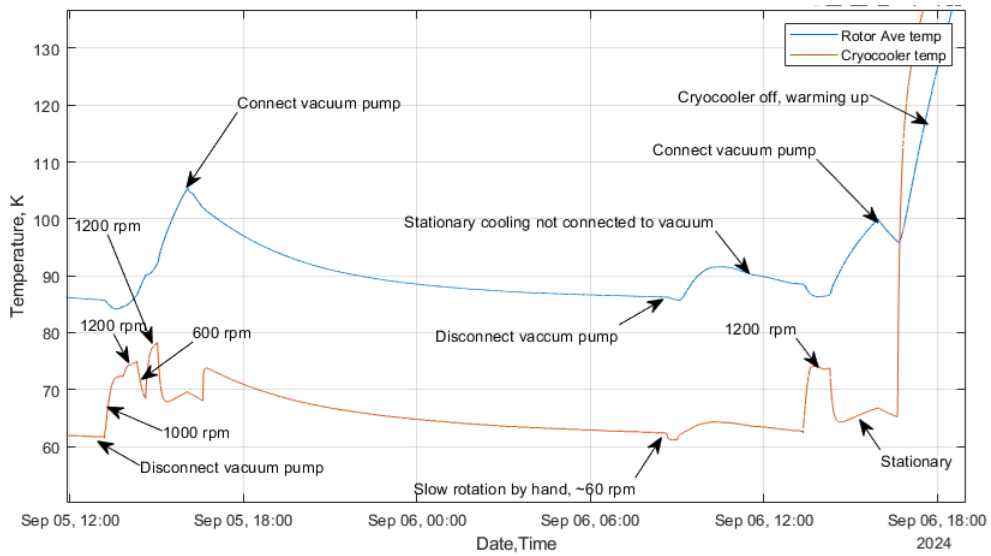

Figure 7. Rotation test with new heat exchanger showing cryocooler temperature and rotor average temperature for a variety of rotation speeds and with the vacuum pump connected while stationary.

rpm, increasing to 1200 rpm. Rotation was briefly reduced to 600 rpm before returning to 1200 rpm. The rotation was then stopped, and temperatures continued to rise. As soon as the vacuum was reconnected and pumping resumed, the temperatures dropped to their previous level, showing that the vacuum was a significant contributor to the temperature rise when rotating. Slow turning by hand disturbed the gravitational currents resulting in reduced cryocooler and rotor temperatures. Stationary with a static vacuum again saw poorer performance than with the vacuum pump on, then a run at 1200 rpm showed lower rotor temperatures plus higher cryocooler temperatures. Finally, the vacuum pump was reconnected dropping the temperatures before the cryocooler was turned off and the rotor warmed up. A later static vacuum test showed that the vacuum deteriorating from $4x10^{-6}$ mbar to $1.6x10^{-4}$ mbar in 30 minutes. With the small volume of the cryostat, this represented a leak rate of $3.5x10^{-7}$ mbar l/s.

Conductance during the test is shown in Figure 8. At 1000 rpm, the conductance was 1.9 W/K, an improvement on the previous 1.76 W/K, possibly due to the greater area for heat transfer. Increasing the speed to 1200 rpm improved the conductance to a maximum of 2.2 W/K, and 2 W/K on a repeat 1200 rpm. Spinning slowly at 600 rpm, resulted in a conductance of 1 W/K. Finally, turning by hand at approximately 60 rpm achieved 0.7 W/K conductance which was smaller than the stationary conductance and could be expected as the slow rotation would have disrupted the gravitationally induced flow inside the rotor.

3. Prediction of performance at full rpm

The rotating tests were performed at a maximum of 1200 rpm where a conductance of 2.2 W/K was achieved. The full speed of the operating motor is intended to be 4500 rpm. The pumping has a mass flow rate that is approximately proportional to the rotational speed. A curve fit to the data points for 600, 1000 and 1200 rpm, predicts a conductance of 9.2 W/K for 4500 rpm, which for 20 W of heat load, would correspond to a temperature difference of 2.2 K between the cold head of the cryocooler and the rotor average temperature (temperature at the coils). This compares very favourably with the conduction cooled approach which must conduct heat across multiple contact resistances and over a significant distance, in the order of 0.4 m for a motor of that length.

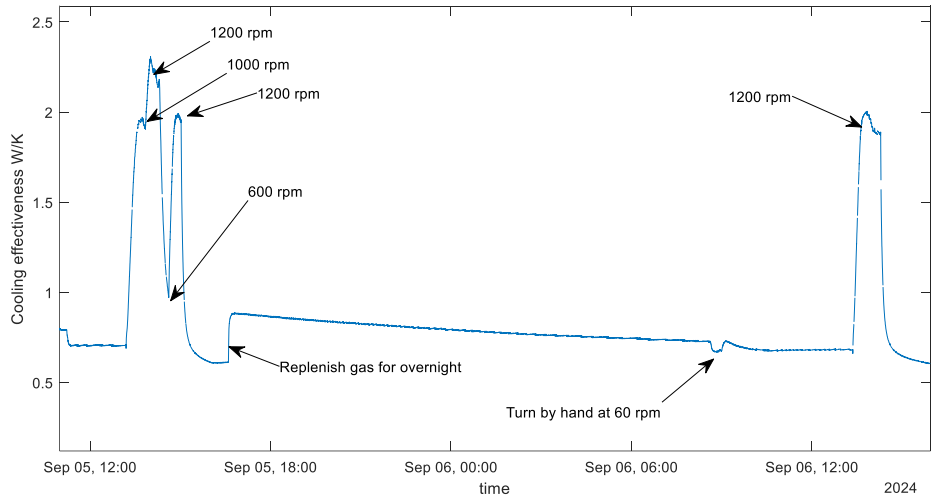

Figure 8. Conductance between cryocooler and rotor average test during rotation test with new heat exchanger. These figures were calculated using the rotor and cryocooler temperatures plus the measured cooling curve of the test DS30 cryocooler.

4. Discussion and Conclusions

The concept of incorporating a circulating pump and helium gas to the centre of a rotor has been shown to be an effective way to transfer heat from the rotor to the cold heat exchanger. The drawbacks of this concept are that a rotary gas seal is required, and that cooling is not as effective while stationary as it is while rotating. However, the advantages of the concept are the ability of helium gas to transport heat a long distance with little temperature rise is of great use for long rotors where the distance between the coils and the cold heat exchanger is large. Additionally, the direction of the gas flow can mean that the higher heat loads are intercepted at the end of the flow path, leading to a lower coil temperature. The pumped rotor concept lends itself to replacing the cryocooler with a heat exchanger cooled by a circulated cryogen such as high-pressure helium gas. This method retains the ability to have a high-pressure circulation circuit with a low-pressure in the rotor, enabling the rotary seal to only have a low-pressure difference, enabling lip or ferrofluidic seals.

Acknowledgments

This research was supported by the Ministry of Business, Innovation and Employment, New Zealand under the Advanced Energy Technology Platform program “High power electric motors for large scale transport” contract number RTVU2004

References

[1] Umemoto K, Aizawa K, Yokoyama M, Yoshikawa K, Kimura Y, Izumi M, Ohashi K, Numano M, Okumura K, Yamaguchi M, Gocho Y and Kosuge E 2010 Development of 1 MW-class HTS motor for podded ship propulsion system *J. Phys. Conf. Ser.* **234**

[2] Grilli F, Benkel T, Hänisch J, Lao M, Reis T, Berberich E, Wolfstädter S, Schneider C, Miller P, Palmer C, Glowacki B, Climente-Alarcon V, Smara A, Tomkow L, Teigelkötter J, Stock A, Büdel J, Jeunesse L, Staempflin M, Delautre G, Zimmermann B, Woude R Van Der, Perez A, Samoilenkov S, Molodyk A, Pardo E, Kapolka M, Li S and Dadhich A 2020 Superconducting motors for aircraft propulsion: The Advanced Superconducting Motor Experimental Demonstrator project *J. Phys. Conf. Ser.* **1590** 1–8

[3] Gamble B, Snitchler G and Macdonald T 2011 Full power test of a 36.5 MW HTS propulsion motor *IEEE Trans. Appl. Supercond.* **21** 1083–8

[4] Snitchler G, Gamble B and Kalsi S S 2005 The performance of a 5 MW high temperature superconductor ship propulsion motor *Appl. Supercond. IEEE Trans.* **15** 2206–9

[5] Spaven F, Liu Y, Bucknall R, Coombs T and Baghdadi M 2021 Thermal design of superconducting cryogenic rotor: Solutions to conduction cooling challenges *Case Stud. Therm. Eng.* **28** 101423

[6] Frank M, Frauenhofer J, Gromoll B, Van Haßelt P, Nick W, Nerowski G, Neumüller H W, Häfner H U and Thummes G 2004 Thermosyphon Cooling System for the Siemens 400kW HTS Synchronous Machine *AIP Conf. Proc.* **710** 859–66

[7] Sato R, Felder B, Miki M, Tsuzuki K, Hayakawa H and Izumi M 2013 Helium-neon gas mixture thermosyphon cooling and stability for large scale HTS synchronous motors *IEEE Trans. Appl. Supercond.* **23** 3–6

[8] Hoffmann J, Canders W R and Henke M 2024 Design Study for a Superconducting High-Power Fan Drive for a Long-Range Aircraft *Energies* **17**

[9] Jeong S, Kim B, Weijers H W, Badcock R A, Jiang Z, Hunze A, Lumsden G, Gschwendtner M, Singamneni S, Caughley A and Glasson N 2021 Holistic approach for cryogenic cooling system design of 3 MW electrical aircraft motors *AIAA Propuls. Energy Forum, 2021* 1–9

[10] Dyson R W, Jansen R H, Duffy K P and Passe P J 2019 High efficiency megawatt machine rotating cryocooler conceptual design *AIAA Propuls. Energy Forum Expo. 2019* 1–15

[11] Caughley A J, Allpress N, Lumsden G, Rogers Rhen N, Gschwendtner M A and Jeong S 2024 A cooling method for the rotor of a superconducting motor - CERN 1.pdf *IOP Conf. Ser. Mater. Sci. Eng.* **1301**

[12] Caughley A J, Allpress N, Ngoc L Le, Lumsden G and Rehn N R 2024 Proof-of-Concept Testing for Integrating a Stationary Cryocooler into the Rotor of a Superconducting Motor *Cryocoolers 23* **23** 435–43